Russian Chemical Reviews **78** (12) 1111 – 1121 (2009) © 2009 Russian Academy of Sciences and Turpion Ltd

DOI 10.1070/RC2009v078n12ABEH004073

Theoretical description and predictions of the properties of superheavy nuclei

A Sobiczewski

Contents

I.	Introduction	1111
II.	Theoretical methods	1111
III.	Role of the shell structure in the stability of heaviest nuclei	1112
IV.	Calculated shell correction	1113
V.	Illustration of the shell structure	1114
VI.	Illustration of the results on the properties of heaviest nuclei	1115
VII.	Conclusion	1119

Abstract. Theoretical descriptions of superheavy atomic nuclei are shortly reviewed and illustrated by their results. Such properties of these nuclei as their shapes, masses, fission barriers, decay modes, decay energies, half-lives, are discussed. Special attention is given to the shell structure of the nuclei, due to which they exist. The role of the physical studies of the superheavy nuclei for the chemical research on the superheavy elements and, more generally, the relationship between these two kinds of investigation is underlined. This stresses the importance of close cooperation between physicists and chemists, experimentalists and theoreticians, in these studies. The bibliography includes 111 references.

I. Introduction

Superheavy elements (SHE) are the elements which exist only due to the shell structure of the nuclei of their atoms. Almost all calculations of this structure, done by various methods, indicate that these are the elements with the atomic number $Z \geqslant 104$, *i.e.*, the transactinide elements. Chemical studies of these elements have already quite a rich tradition. These studies constitute a continuation of the research of D I Menedeleev on the Periodic Table of Elements. This continuation is important and fascinating as it extends the studies of the Periodic Table to an exotic region of very heavy elements, where large relativistic effects appear and significantly modify the properties of the elements.

There is a close relationship between chemical and physical studies of SHE. As these elements have not been found in nature (and one, generally, does not know if they may exist in the Earth), before chemical studies, they have to be produced artificially in a laboratory. And this is done by physical methods (nuclear reactions). Thus, chemical research depends on the physical studies. But also *vice versa*, chemical studies are very helpful to the physical ones, *e.g.*, they supply us with one of the methods of the identification of the atomic number of an element synthesized by physical methods. Hence, the studies of SHE is the field of the joint research of physicists and chemists, experimentalists and theoreticians. Only common efforts of these four groups of researchers are effective and lead to a fast progress of our knowledge in this field.

Physical studies of superheavy nuclei (SHN) constitute presently a large branch of nuclear physics. Both experimental and theoretical reserch is being done. More than 80 superheavy nuclei of 14 superheavy elements with $Z = 104 - 118$ (with the only exception of $Z = 117$) have been already synthesized. Many properties of these nuclei, such as mode of α decay (mainly a decay and spontaneous fission), decay energy, half-life, cross section for their synthesis and other, have been already learned. This knowledge allow one to improve or construct new theoretical models which, in turn, allow deeper understanding of experimental results and prediction for SHN not yet observed or for new properties of SHN already seen.

Experimental studies of SHN have been described in many papers (*e.g.*, Refs 1 – 16, a large number of which are reviews). The objective of this article is to give a short review of theoretical studies of SHN illustrated by examples of the results of these studies.

II. Theoretical methods

Mainly two approaches are used in the theoretical description of nuclei. One, traditional, is a macroscopic – microscopic (macro – micro) approach (*e.g.*, Refs 17 – 21), the other, more recent, comprises purely microscopic, self-consistent methods. Both remain within the approach of the mean nuclear field.

A Sobiczewski Department of Theoretical Physics, Andrzej Soltan Institute for Nuclear Studies, Hoza str. 69, 00-681 Warsaw, Poland. Fax (48-22) 621 60 85, tel. (48-22) 553 22 78, e-mail: Sobicz@fuw.edu.pl

Received 6 May 2009
Uspekhi Khimii **78** (12) 1200 – 1210 (2009)

In the macro–micro method, the energy (mass), E, of a nucleus at a given deformation (β_λ) is composed of two parts,

$$E(\beta_\lambda) = \tilde{E}(\beta_\lambda) + \delta E_{\rm sh}(\beta_\lambda), \quad (1)$$

where $\tilde{E}(\beta_\lambda)$ is the macroscopic and $\delta E_{\rm sh}(\beta_\lambda)$ is the microscopic part of the energy. The macroscopic part, which smoothly depends on the proton Z and neutron N numbers, does not include effects of the shell structure of a nucleus. It is usually described by such models as the liquid-drop one (*e.g.*, Refs 22 and 23) or the Yukawa–plus-exponential model.[24] The microscopic part describes shell effects. This is usually based on a realistic single-particle nuclear potential (most often the Woods–Saxon potential[25] and is constructed from the single-particle energy spectra by the Strutinski procedure.[26,27]

The self-consistent methods use calculations of the Hartree–Fock type with effective density-dependent interactions of the zero-range (Skyrme) type (*e.g.*, see Refs 28 and 29) or of the finite-range (Gogny) type (*e.g.*, Refs 30 and 31). The relativistic mean field approach[32–34] intensively used in recent years for the description of nuclear properties also belongs to purely microscopic methods. The self-consistent calculations are more complex and time-consuming than the macro–micro ones. Illustrations of the results obtained within both of these approaches and a comparison between them may be found in a number of papers (*e.g.*, Refs 35 and 36). In this paper, we will mainly use the macro–micro approach for the illustration of the description of heavy and superheavy nuclei.

III. Role of the shell structure in the stability of heaviest nuclei

The shell structure is important for all nuclei. Its role for the heaviest ones is, however, essential because these nuclei would not exist without this structure,[37] as already mentioned in the Introduction. In this Section, we will illustrate this role in a number of properties of heavy and superheavy nuclei.

The effects of the shell structure of real nuclei may be estimated by comparing measured properties of these nuclei with those calculated within macroscopic models, in which the nuclei have no shell structure. Figure 1 taken from Ref. 37 illustrates the shell effects in masses of heaviest nuclei. The effect is the difference between the experimental value of mass and the value calculated within a model that does not include the shell structure (*e.g.*, liquid-drop model). One can see that the shell effect, $(M_{\rm exp} - \tilde{M})$, is negative (*i.e.*, it stabilizes the nuclei) and decreases (increases in its absolute value) with increasing atomic number Z, down to about -5 MeV for the heaviest even–even nuclei ^{260}Sg ($Z = 106$) and ^{264}Hs ($Z = 108$) known at the time when early studies of shell effects in the properties of heaviest nuclei were performed. The effect of the known deformed shell at the neutron number $N = 152$ is clearly seen in the results for Cf, Fm and No ($Z = 102$) isotopes. Similarly clear and large shell effects were found in other important properties of heaviest nuclei, such as the α-decay energy (Q_α) and half-life (T_α) or the height of the fission barrier ($B_{\rm f}$).[37]

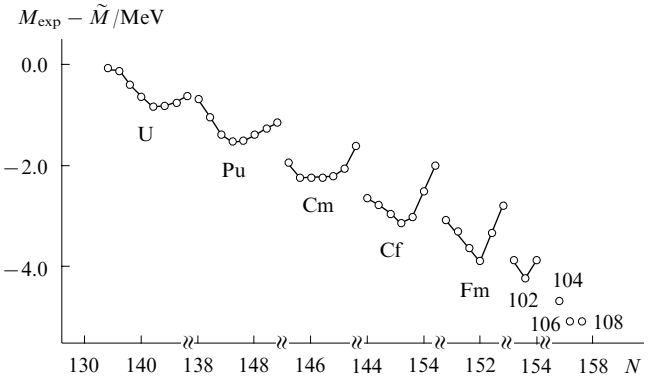


Figure 1. Shell effects in the masses of nuclei.[37]

An especially large effect, up to 15 orders of magnitude, appears in the spontaneous-fission half-life ($T_{\rm sf}$). This is because this quantity is especially sensitive to the shell structure of a nucleus. The effect is illustrated in Fig. 2.[37] The Figure shows the experimental and theoretical values of the logaritm of $T_{\rm sf}$. The theoretical values are calculated by a macroscopic (Yukawa–plus-exponential[24]) model, which does not include any shell structure of a nucleus. Thus, the difference between the two values is just the shell effect in the spontaneous-fission half-life $T_{\rm sf}$. One can see that the effect delays the fission process in all considered nuclei, except only few lightest ones (isotopes of uranium). The delay increases from few orders (plutonium isotopes) to about 15 orders of magnitude for the nucleus ^{260}106 (^{260}Sg), which has the largest Z among the even–even nuclei with measured $T_{\rm sf}$. For such a heavy nucleus like ^{260}106, with $T_{\rm sf}$ of the order of few milliseconds, this extension makes up practically the whole half-life of these nuclei. In other words, they would not exist without shell effects, as already mentioned above.

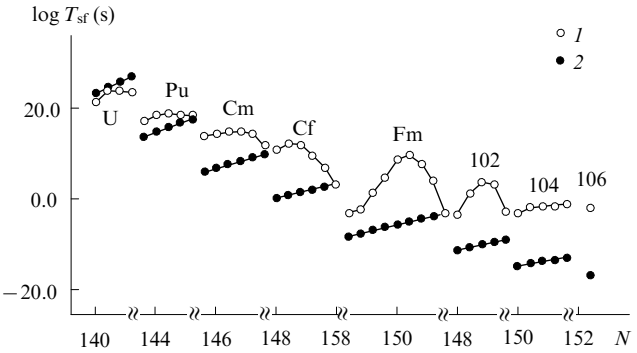


Figure 2. Logarithm of experimental (*1*) and calculated macroscopically (*2*) spontaneous-fission half-lives $T_{\rm sf}$.[37]

The mechanism by which practically the whole half-life of a very heavy nucleus is made up by shell effects is illustrated in Fig. 3. The figure illustrates the spontaneous-fission barrier of the nucleus ^{264}108 (^{264}Hs), *i.e.*, the dependence of the ground-state energy of this nucleus on its quadrupole-deformation parameter β_2. For each β_2, the energy is minimized with respect to the hexadecapole-deformation parameter β_4. The total fission barrier including shell effects, is shown by curve *1* and its smooth part (obtained by the Yukawa–plus-exponential model[24]) is represented by curve *2*. The smooth barrier (curve *3*)

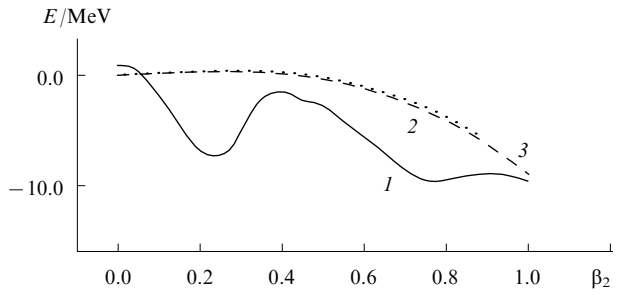


Figure 3. Total fission barrier (*1*) and its macroscopic part obtained by Yukawa–plus-exponential (*2*) and by the liquid-drop (*3*) models, for the nucleus $^{264}108$.[37]

obtained by another macroscopic model [liquid drop, LD (Ref. 22)] is also shown (curve *3*), for comparison. One can see that a significant height (about 6 MeV) of the fission barrier is obtained only after the inclusion of shell effects. Without them, no fission barrier (see curves *2*, *3*) appears.

IV. Calculated shell correction

After the realization that the effects of the shell structure are so large and depend strongly on the proton and neutron numbers (*i.e.*, on the composition of a nucleus), it was important to calculate them for a large region of heaviest nuclei. This should give the idea of which nuclei are characterized by the largest shell effects. Such a calculation has been reported (Fig. 4).[38] The Figure shows a contour map of the shell correction (E_{sh}) to the ground-state energy (or mass) of nuclei in a large region of nuclides with proton number $Z = 82-120$ and neutron number $N = 126-190$. One can see that E_{sh} has three minima in this region. The first one, which is the deepest ($E_{sh} = -14.3$ MeV), is obtained for the doubly magic spherical nucleus ^{208}Pb. The second one ($E_{sh} = -7.2$ MeV) appears at the nucleus $^{270}108_{162}$, which is predicted[39,40] to be a doubly magic deformed nucleus. The third minimum with the same depth ($E_{sh} = -7.2$ MeV) as the second one is obtained for the nucleus $^{296}114_{182}$, which is close to the nucleus $^{298}114_{184}$ predicted[41–43] to be a doubly magic spherical nucleus, the next one to the last experimentally known double-magic

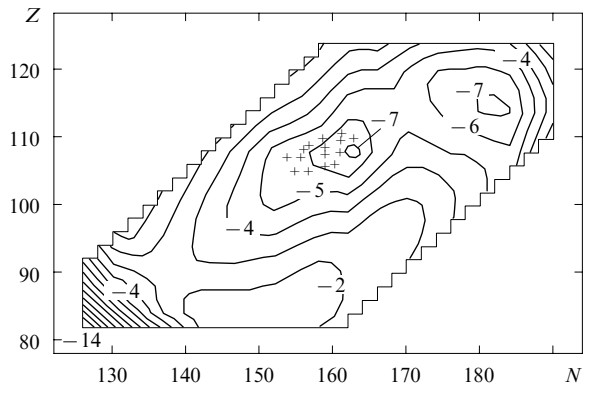


Figure 4. Contour map of the ground-state shell correction energy (E_{sh}/MeV).[38]
Crosses denote heaviest nuclei which were synthesized by the time the figure was plotted.

^{208}Pb. Besides these three minima, there appears a rather wide plateau around the nucleus ^{252}Fm, which, although having a smaller (in absolute value) shell correction ($E_{sh} = -5.2$ MeV) than the nucleus $^{270}108$ (^{270}Hs), may be considered as a nucleus with closed deformed subshells.[39,40]

One can also see in Fig. 4 that some of the already synthesized nuclei profit by 6–7 MeV in their binding energy from the shell correction. Without this profit they could not exist, as already discussed above.

The appearance of the region of nuclei around the second minimum (deformed superheavy nuclei) constitutes probably the main change in our view of stability of heaviest nuclei in the whole history of SHE. Before this, it was believed for a long time that spherical superheavy nuclei predicted to be situated around the third minimum would constitute an island, separated from the usual peninsula of relatively long-lived nuclei by an 'ocean' of full instability. After the appearance of deformed superheavy nuclei, however, the peninsula is expected to be extended, to include also the spherical superheavy nuclei. This is qualitatively illustrated in Fig. 5 taken from Ref. 44.

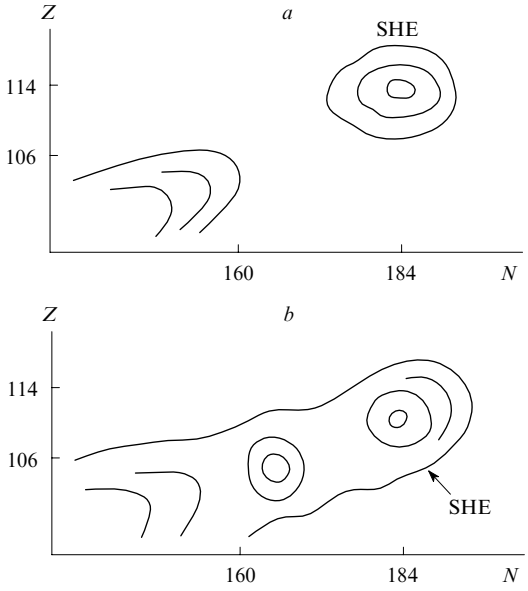


Figure 5. Regions of relatively long-lived heavy nuclei as believed earlier (*a*) and expected presently (*b*).[44]

It may be useful to note that the shell correction given in Fig. 4 is the global one. It is defined as the total gain in energy of a nucleus due to its shell structure. Thus, it is the difference

$$E_{sh}^{glob} \equiv E(\beta_\lambda^0) - \tilde{E}(0), \qquad (2)$$

where $E(\beta_\lambda^0)$ is the energy of the nucleus at its equilibrium deformation (β_λ^0) in the case when the nucleus has the shell structure, while $\tilde{E}(0)$ is its energy in the case of no shell structure. In the latter case (*e.g.*, within the liquid-drop model of the nucleus), the equilibrium deformation is zero. Thus, generally, the global shell correction is the difference between energies of a nucleus at different deformations of it. Due to this, it differs from the local shell correction $\delta E_{sh}(\beta_\lambda)$, which, according to Eqn (1), is given by

$$\delta E_{\rm sh}(\beta_\lambda) \equiv E(\beta_\lambda) - \tilde{E}(\beta_\lambda). \quad (3)$$

For the equilibrium deformation, the difference between the two is

$$E_{\rm sh}^{\rm glob}(\beta_\lambda^0) - \delta E_{\rm sh}(\beta_\lambda^0) = \tilde{E}(\beta_\lambda^0) - \tilde{E}(0), \quad (4)$$

i.e., it is the deformation energy of the macroscopic part of the energy of a nucleus. For heavy nuclei, which are close to instability in the macroscopic models and their macroscopic energy is flat as a function of deformation (see Fig. 3), this difference is small. For spherical nuclei (in particular superheavy ones) it is simply zero.

To compare these both kinds of the shell correction used in literature, we show in Fig. 6 (see Ref. 45) a contour map of the local shell correction. Comparing Fig. 6 with Fig. 4, one can see that the local shell correction is larger by about 2 MeV (in the absolute value) than the global one at the centre of the deformed SHN. For the centre of the spherical SHN (not shown in Fig. 6), both shell corrections are the same, as already stated above.

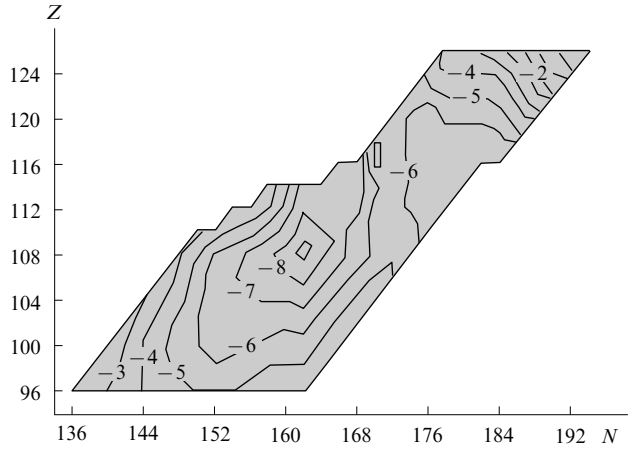


Figure 6. Contour map of the local shell correction, $\delta E_{\rm sh}^{\rm gs}$/MeV calculated at the equilibrium point of the considered nuclei.[45]

V. Illustration of the shell structure

The shell structure of a nucleus is seen in its single-particle spectrum. This is just inhomogeneity of the spectrum, the appearance of shells (regions of a larger density of the single-particle energy levels) separated by energy gaps.

Since large shell corrections to energy (mass) of a nucleus are related to large energy gaps in the single-particle spectra, it is interesting to consider the single-particle spectra of the nuclei ^{208}Pb, ^{270}Hs, and ^{298}114, for which the three minima of the shell correction $E_{\rm sh}$ are shown in Fig. 4. These spectra for protons and neutrons are shown in Figs 7 and 8.[46] One can see (Fig. 7) large energy gaps at $Z = 82$ (in the spectrum of ^{208}Pb), at $Z = 108$ (in ^{270}Hs), and at $Z = 114$ (in ^{298}114). In the spectrum of ^{270}Hs, a low density of the levels extends from $Z = 106$ to $Z = 110$. For neutrons (Fig. 8), apart from the large energy gap obtained at $N = 162$ in the spectrum of ^{270}Hs, a smaller gap at $N = 152$ is also seen. All these factors are reflected in the shell correction to the energy $E_{\rm sh}$ shown in Fig. 4.

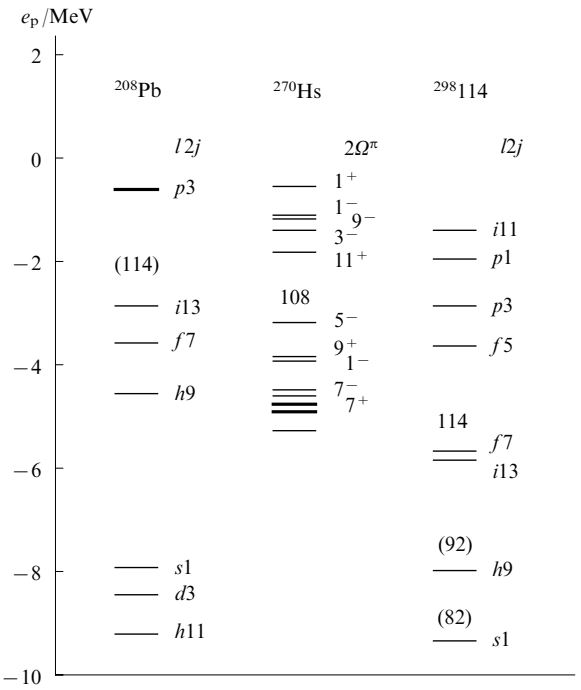


Figure 7. Single-particle proton levels calculated for the doubly magic nuclei ^{208}Pb, ^{270}Hs, and ^{298}114.
Here and in Fig. 8, the spectroscopic symbol for orbital angular momentum (l) and total spin (multiplied by two, $2j$) are given at each level of the spherical nuclei ^{208}Pb and ^{298}114. Projection of spin (multiplied by two, 2Ω) and parity (π) are shown at each level of the deformed nucleus ^{270}Hs.[46]

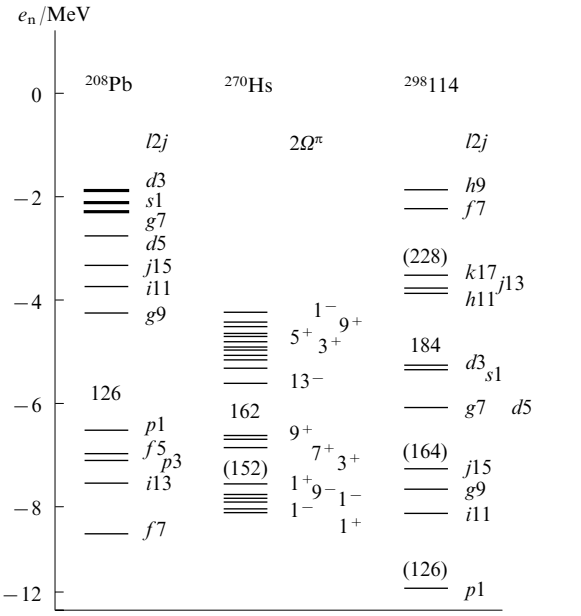


Figure 8. Single-particle neutron levels calculated for the doubly magic nuclei ^{208}Pb, ^{270}Hs and ^{298}114.[46]

VI. Illustration of the results on the properties of heaviest nuclei

In this Section, we will illustrate some theoretical results for the properties of heavy and superheavy nuclei. The results have been mainly obtained within a macroscopic–microscopic approach.

1. Nuclear shapes

To find the equilibrium shape of a nucleus, one minimizes its energy in the deformation parameters β_λ. The shapes of heaviest nuclei are found to be axially symmetric.[47] Thus, they can be described by the usual deformation parameters β_λ, appearing in the following expression for nuclear radius (in the intrinsic frame of reference) in terms of spherical harmonics $Y_{\lambda 0}(\vartheta)$,

$$R(\vartheta) = R_0(\beta_\mu)\left[1 + \sum_\lambda \beta_\lambda Y_{\lambda 0}(\vartheta)\right], \tag{5}$$

where the dependence of R_0 on β_μ is determined by the volume-conservation condition.

A macro–micro analysis of the equilibrium deformations has shown[48] that it is sufficient to consider the multipolarities up to $\lambda = 8$. The contribution of $\lambda = 9$ and 10 is already negligible. The odd multipolarities $\lambda = 3$, 5 and 7 contribute only to the deformations of light isotopes of elements around radium.[48] Thus, the 4-dimensional deformation space $\{\beta_\lambda\}$, $\lambda = 2$, 4, 6 and 8 has been found to be sufficient for almost all nuclei in the considered region of heaviest nuclei, in which we are usually interested, in particular for all superheavy nuclei.[38]

The shapes of the nuclei are illustrated in Fig. 9.[49] The symmetry axes (Oz) of the nuclei have the horizontal orientation in the Figure. One can see that the shapes vary quite significantly with Z and N. Some of the nuclei are thicker in their equatorial plane, some are thinner (necking), some ($Z > 120$) show a tendency to be oblate. Numerical values of the equilibrium deformations β_λ^0 were reported.[50, 51]

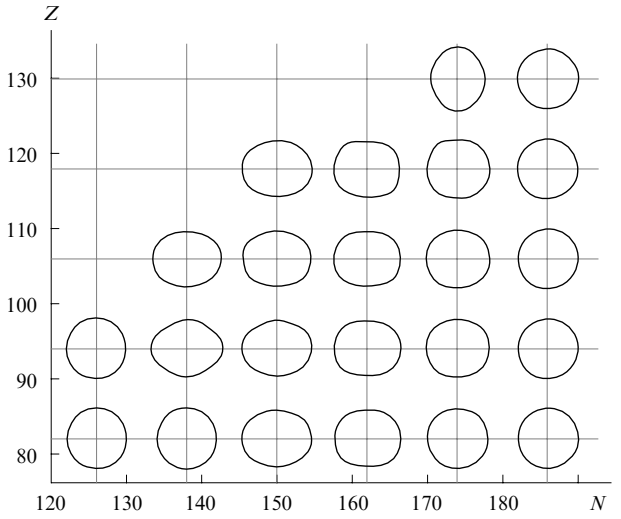


Figure 9. Shapes of nuclei plotted for a wide region of Z (82–130) and N (126–190).[49]

2. Masses and α-decay energies

Mass is a basic property of a nucleus and it should be described as accurately as possible. Figure 10 shows the difference between the calculated and experimental masses of nuclei with $Z = 84$–108.[50] A large, seven-dimensional deformation space $\{\beta_\lambda^0\}$, $\lambda = 2, 3, \ldots, 8$, has been used in the calculations. So large space is used, because the considered region of nuclei covers relatively light nuclei (starting from polonium, $Z = 84$) for which the odd-multipolarity deformations, $\lambda = 3$, 5, 7, play a role, as has been mentioned above. One can see that the discrepancy between the calculated mass M_{th} and the experimental one M_{exp} is roughly contained within the range of about ± 0.5 MeV. The calculated masses show a very good isotopic dependence. This is especially well seen in the long chain of masses of well deformed plutonium nuclei. From masses of Cm, Cf and Fm, one can see that the effect of the deformed shell at $N = 152$ on the mass is well reproduced. One cannot say, however, if this is also the case for a stronger deformed shell at $N = 162$ predicted by theory, because the masses of nuclei with N around 162 are not yet measured.

It is of interest to compare the accuracies of description of masses of the heaviest nuclei attained within various approaches. Figures 11 and 12 (Ref. 52) show the differences $M_{\text{th}} - M_{\text{exp}}$ where the theoretical value was determined using a semi-empirical (SE), two macro–micro (Heaviest Nuclei, HN, and Thomas–Fermi, TF) and purely microscopic (Harthree–Fock, HF) approaches. The semi-empirical description[53] uses a shell model with 15 adjustable parameters specially adapted to describe the masses of nuclei with proton numbers located between the known magic number $Z = 82$ and the assumed one $Z = 126$ and with neutron numbers contained between the known magic number $N = 126$ and the assumed one $N = 184$. The macro–micro approximation HN (Ref. 54) is the same model that was used to calculate the masses of Fig. 10. The TF theory is of the macro–micro model in which the macroscopic part of mass was obtained with the use of the Thomas–Fermi approximation.[55] Finally, the microscopic model HF (Hartree–Fock–BCS approach[56]) in which a 10-parameter Skyrme effective interaction has been used to obtain the mean field and a 4-parameter δ-function has been taken to describe the pairing interaction. Experimental masses used in Figs 10–12 have been taken from Ref. 57. One can see in Fig. 11 that the discrepancy between the theoretical and experimental masses is roughly contained within ± 0.5 MeV for three of the considered models. Only for the HF approach, it is larger, up to about 1 MeV. The best agreement is obtained for the SE and HN approaches.

To make a quantitative comparison of the discussed approaches for a large number of heavy nuclei, the root-mean-square deivations of masses were calculated for 238 nuclei (having reliably determined experimental masses[57]) from the region of heaviest nuclei with $Z \geqslant 84$ and $N \geqslant 126$. The rms deviations of the masses (in keV) calculated within the SE, HN, TF, FRLDM, and HF models from the experimental masses are given below.[52]

Model	SE	HN	TF	FRLDM	HF
ΔM /keV	145	370	482	705	705

In addition to the four discussed models, the Finite-Range Liquid Drop Model (FRLDM)[58] was also included for comparison. This is a macro–micro model, like the HN and TF models. One can see that the smallest deviations

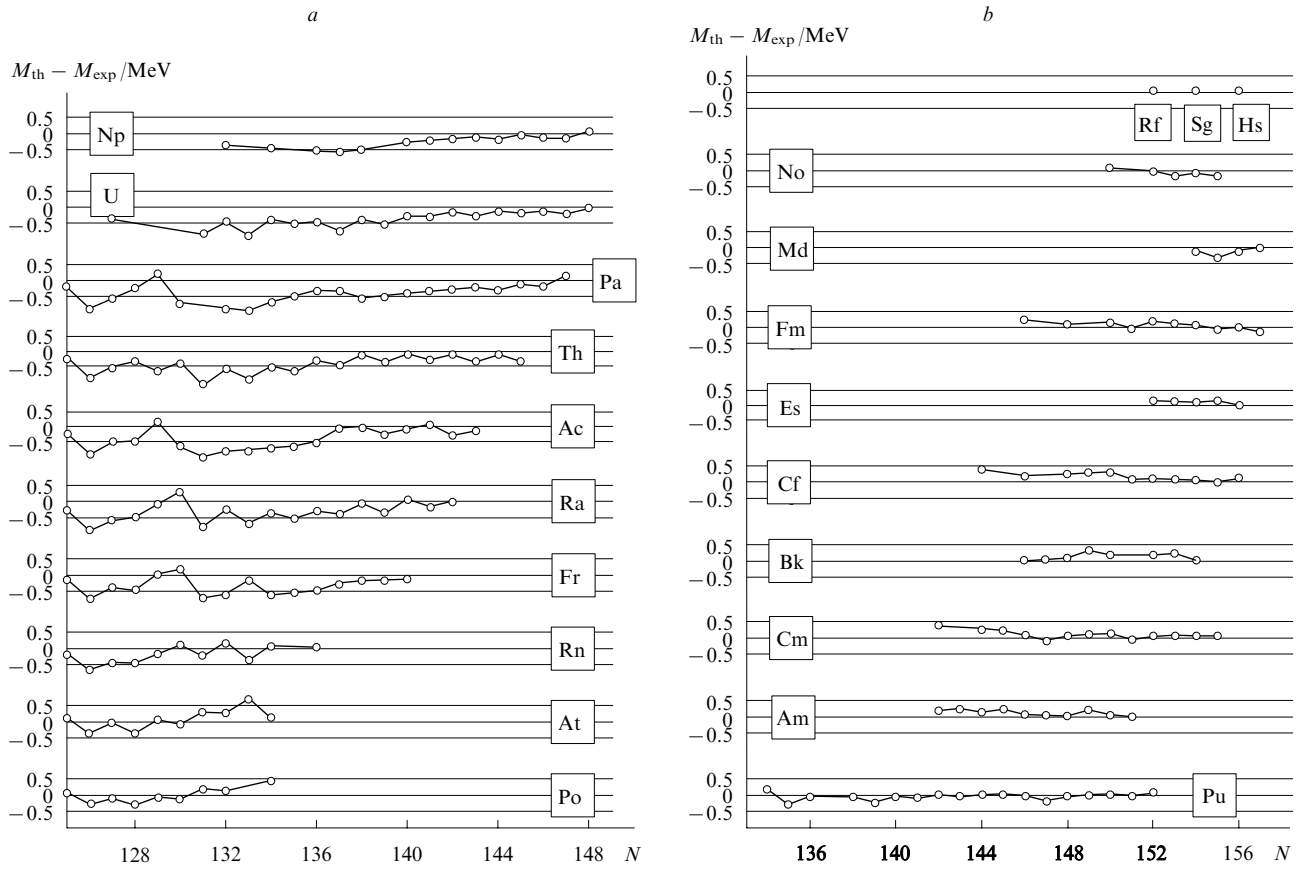


Figure 10. Differences between calculated and measured masses of nuclei with proton numbers $Z = 84-93$ (*a*) and $Z = 94-108$ (*b*).[50]

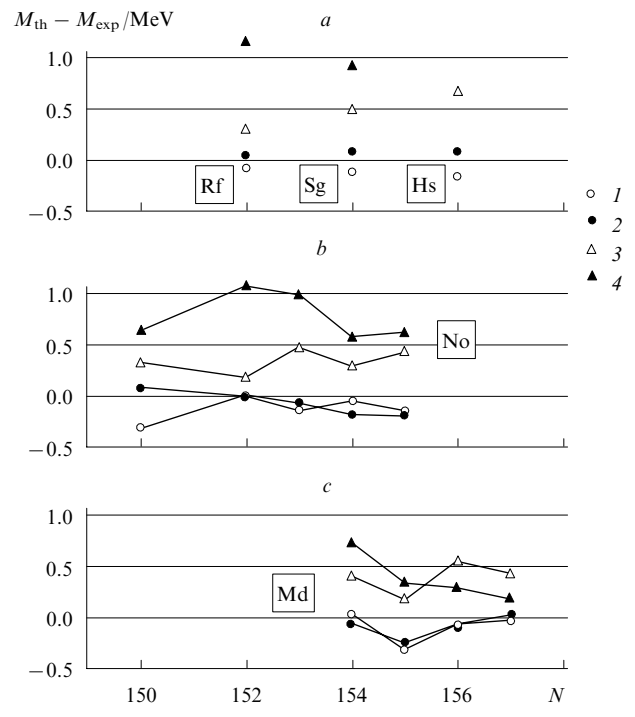


Figure 11. Differences between the SE (*1*), HN (*2*), TF (*3*) and HF (*4*) masses and experimental ones for heaviest nuclei with $Z = 101-108$: Rf, Sg, Hs (*a*), No isotopes (*b*) and Md (*c*).
For designations, see the text.[52]

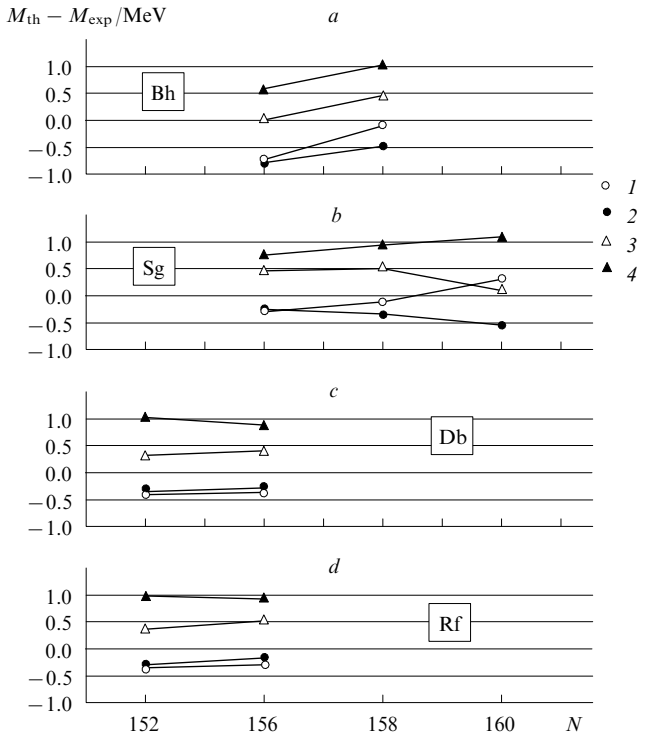


Figure 12. Differences between the SE (*1*), HN (*2*), TF (*3*) and HF (*4*) masses and experimental ones for odd and odd–odd nuclei with $Z = 104-107$: Bh (*a*), Sg (*b*), Db (*c*), and Rf (*d*) isotopes.[52]

were obtained for the SE and HN models. This is probably due to special adaptation of them to description of heaviest nuclei, while the others are adapted to describe masses of all nuclides.

The α-decay energies directly related to masses are described with a similar accuracy.[59]

3. Fission barriers

A study of the (static) fission-barrier height (B_f^{st}) of heaviest nuclei is motivated by the importance of this value in calculations of cross sections σ for the synthesis of these nuclei (*e.g.*, see Refs 60–72). The height B_f^{st} is a decisive quantity in the competition between neutron evaporation and fission of a compound nucleus during its cooling. A large sensitivity of σ to B_f^{st} enhances the need for accurate calculations of B_f^{st}. For example, a change in B_f^{st} by 1 MeV may result in a change of σ by about one order of magnitude or even more.[64] The basic role in the calculations of B_f^{st} is played by the deformation space used. Up to the present, the height B_f^{st} has been mostly studied in the case of axial symmetry of a nucleus (*e.g.*, Refs 73–78). Studies taking into account non-axial degrees of freedom were less frequent (*e.g.*, 47, 79 and 80).

Here we will illustrate recent results obtained for the barriers B_f^{st} for heavy and superheavy nuclei, stressing the importance of non-axial deformations taken into account in the calculations of this quantity.

First, consider an example of the static fission barrier obtained in the case of the axial symmetry of a nucleus. Figure 13 shows such a barrier for the superheavy nucleus $^{278}112$ (Ref. 81). One can see that a rather high barrier is obtained for this very heavy nucleus, which is entirely created by effects of the shell structure in the energy of this nucleus. Without this structure (see macroscopic part of the energy, curve *1*), no barrier is obtained (see Fig. 3, similarly to curves *2* and *3* for a lighter nucleus). The largest shell correction to the macroscopic part of the energy (about 6 MeV) was obtained at the (deformed) equilibrium point, smaller values (about 1.8 MeV) were found for the first saddle point and the smallest values (about 0.5 MeV) were found for the second saddle point. Significant shell corrections at the saddle points (appearing as energy maxima in Fig. 13) are worthy of notice as these corrections are quite often neglected in various estimates of the static fission barriers of superheavy nuclei. In the Figure, the dependence of the energy of the nucleus on the deformation β_2 is plotted. However, at each value of β_2, the energy is minimized in the β_4, β_6 and β_8 degrees of freedom. The barrier height B_f is the difference between the energy at the highest saddle point and that at the equilibrium point. Thus, B_f depends on the two different configurations of a nucleus: the saddle-point configuration and the equilibrium one.

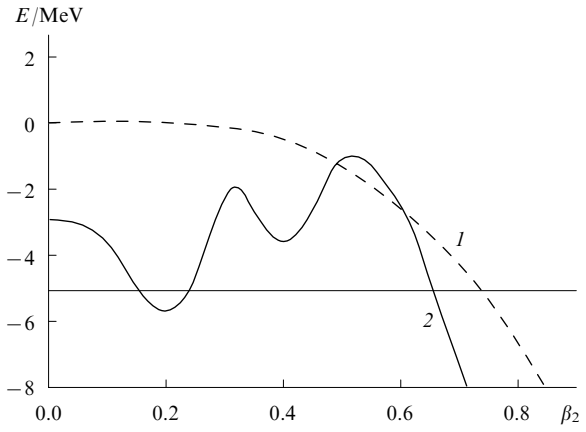


Figure 13. Static spontaneous-fission barrier calculated for the nucleus $^{278}112_{166}$ taking into account only macroscopic (*1*) and total (*2*) energy.[81]

Figure 14 (see Ref. 82) gives a contour map of B_f^{ax} calculated for a large region of nuclei in the case of the axially symmetric shapes. One can see that the largest height B_f^{ax} (about 8.5 MeV), is obtained in the region of nuclei with $Z \approx 99$ and $N \approx 152$. This is connected, to a large extent, with a large shell correction in the ground state of these nuclei (mainly due to the deformed subshell closure at $N = 152$, see, *e.g.*, Ref. 45). Another region of a large B_f^{ax} (about 7 MeV) is obtained for the nuclei with $Z \approx 116$ and $N \approx 180$. In this region, the large B_f is again due to a large shell correction in the ground state of these nuclei, which is connected here with the spherical shell closure at $N = 184$ (*e.g.*, see Ref. 45). Relatively small B_f are obtained in the region of the neutron number $N \approx 168$.

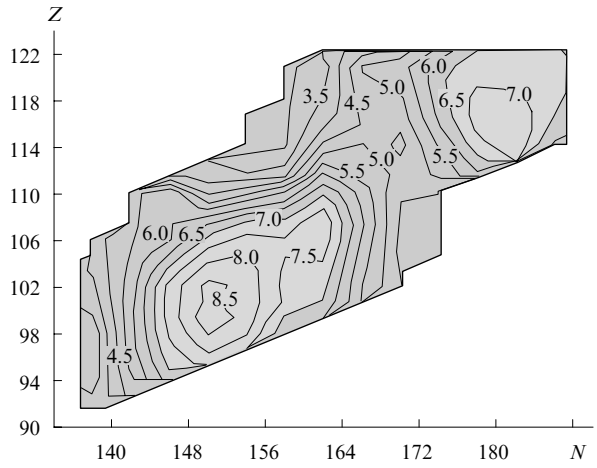


Figure 14. Contour map of the fission-barrier height (B_f^{ax} /MeV) in the case of the axially symmetric shapes.[82]

The influence of non-axial shapes of a nucleus on the barrier height B_f^{st} has been studied in a number of papers (*e.g.*, see Refs 83–87). Figure 15 illustrates this influence for the nucleus ^{250}Cf (Ref. 83). Here, the 5-dimensional deformation space is used. This is specified by the following expression for the nuclear radius $[R(\theta,\varphi)]$ (taken in the intrinsic frame of reference) in terms of spherical harmonics ($Y_{\lambda\mu}$)

$$R(\theta,\phi) = R_0\left\{1 + \beta_2\left[\cos\gamma\, Y_{20} + \frac{1}{\sqrt{2}}\sin\gamma\, Y_{22}\right] + \right. \qquad (6)$$

$$\left. + \beta_4 Y_{40} + \beta_6 Y_{60} + \beta_8 Y_{80}\right\},$$

where $\gamma \equiv \gamma_2$ is the Bohr quadrupole non-axiality parameter, and the dependence of R_0 on the deformation parameters is determined by the volume-conservation condition. In the Figure, the potential energy minimized in β_4, β_6, β_8 is projected on the plane ($\beta_2\cos\gamma$, $\beta_2\sin\gamma$). One can see that the inclusion of non-axial shapes decreases the potential

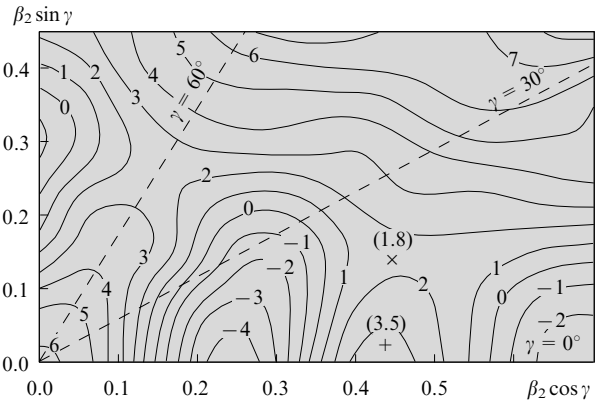


Figure 15. Contour map of the potential energy (MeV) of the nucleus ^{250}Cf taking into account the nonaxial shapes.
The position of the saddle point is marked by the symbol '+' when axial symmetry of the nucleus is assumed, and by the symbol '×', when non-axiality is taken into account. Numbers in parentheses specify the values of the energy at these points.[83]

energy at the saddle point by 1.7 MeV. As non-axial shapes do not decrease the potential energy at the equilibrium point, they decrease the barrier height B_f by the same amount of 1.7 MeV. Only after the inclusion of this decrease, the calculated barrier height B_f becomes close to the measured value (5.6 ± 0.3) MeV.[88] The mechanism by which the quadrupole non-axiality decreases the barrier height B_f has been studied.[89]

A contour map of the reduction $\delta B_f^{\gamma_2}$ of the barrier height B_f due to the non-axial deformation γ_2 is given in Fig. 16. As for all nuclei we investigated, the equilibrium deformation is axially symmetric, the reduction $\delta B_f^{\gamma_2}$ is the reduction of the energy at the saddle point. One can see that the map of Fig. 16 is rather complex. This is characteristic of effects related to the shell structure of nuclei, which changes rather fast from one nucleus to another. The largest reduction of the barrier height $\delta B_f^{\gamma_2}$ is about 2 MeV and appears in two regions of the nuclei: one for nuclei with

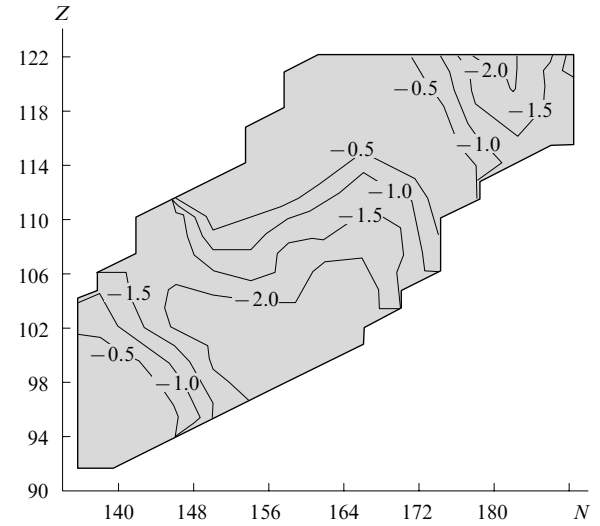


Figure 16. Contour map of the reduction in the fission-barrier height ($\delta B_f^{\gamma_2}$/MeV) due to non-axial quadrupole deformation γ_2.[82]

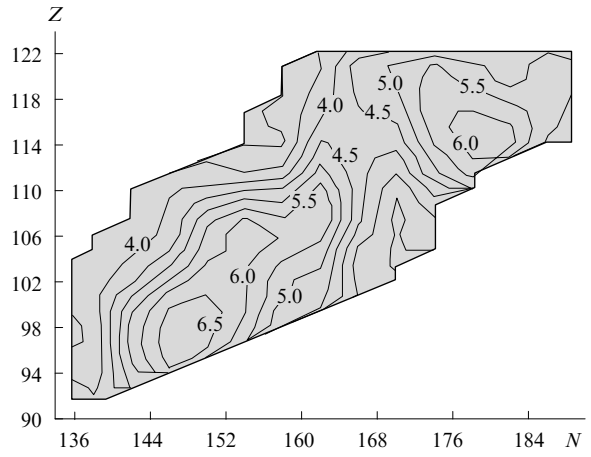


Figure 17. Contour map of the fission-barrier height ($B_f^{\gamma_2}$/MeV) for heavy nuclear after the inclusion of non-axial quadrupole deformation γ_2.[82]

$Z \approx 100$ and $N \approx 158$ and the other with $Z \approx 122$ and $N \approx 180$.

Finally, Fig. 17 shows the barrier height after the inclusion of the effect of γ_2:

$$B_f^{\gamma_2} = B_f^{ax} + \delta B_f^{\gamma_2}.$$

One can see that two regions of nuclei with the largest $B_f^{\gamma_2}$ appear: one with $Z \approx 98$ and $N \approx 148$ ($\sim$6.5 MeV) and the other with $Z \approx 115$ and $N \approx 180$ ($\sim$6.0 MeV). The smallest barriers are obtained for nuclei with $N \approx 168$.

4. Half-lives

Mainly two decay modes govern the stability of heaviest nuclei: α decay and spontaneous fission. Half-lives corresponding to these modes are shortly discussed here.

a. α-Decay

Alpha-decay half-lives are usually calculated with the use of phenomenological formulae (*e.g.*, see Refs 90–93). A simple 7-parameter formula of Viola and Seaborg[90] has been used most frequently for a long time (*e.g.*, Refs 39, 94–99). Recently, an even simpler, 5-parameter formula has been proposed.[100] The formula reads

$$\log_{10} T_\alpha^{ph}(Z,N) = aZ[Q_\alpha(Z,N) - \bar{E}_i]^{1/2} + bZ + c, \qquad (7)$$

where the parameters are $a = 1.5372$, $b = -0.1607$, $c = -36.573$; and the parameter $\bar{E}_i$ (average excitation energy of a state of the daughter nucleus, to which α-decay goes) is

$\bar{E}_i = 0$, if Z, N are even;
$\bar{E}_i = \bar{E}_p = 0.113$ MeV, if Z is odd, N is even;
$\bar{E}_i = \bar{E}_n = 0.171$ MeV, if Z is even, N is odd;
$\bar{E}_i = \bar{E}_p + \bar{E}_n$, Z, N are odd;

The above values of the five parameters a, b, c, E_p and E_n have been obtained by adjustment of them to experimental values of T_α (Ref. 101) with the use of experimental values of Q_α.[102] Here, 61 even–even, 45 odd–even,

55 even–odd and 40 odd–odd nuclei (*i.e.*, altogether 201 nuclei) with $Z = 84-111$ and $N = 128-161$ for which both values Q_α and T_α had been measured were used. For fitting details, see Ref. 100.

b. Spontaneous fission

Spontaneous fission is a complex process. Even a detailed knowledge of the potential energy of a nucleus, *i.e.*, of the dependence of this energy on various kinds of the deformation of a nucleus, is not sufficient. Additionally, a detailed knowledge of the mass parameters, *i.e.*, the inertia of a nucleus against various kinds of the deformation, is needed. Only with these, a realistic description of the spontaneous fission of nuclei may be obtained.[103]

Figure 18 shows an example of half-lives calculated for isotopes of darmstadtium (Ds, $Z = 110$).[104] The calculations are done for both decay modes of heaviest nuclei: α decay (curve *1*) and spontaneous fission (dots *2*), and the results are compared with experimental values. The latter were taken from Ref. 105 for $^{267}110$, Ref. 106 for $^{269}110$, Ref. 107 for $^{271}110$, and Ref. 108 for $^{273}110$. One can see that the calculations correctly predicted the proper values of the half-lives and the mode of decay, *i.e*, the fact that the nuclei really undergo α decay and not fission.

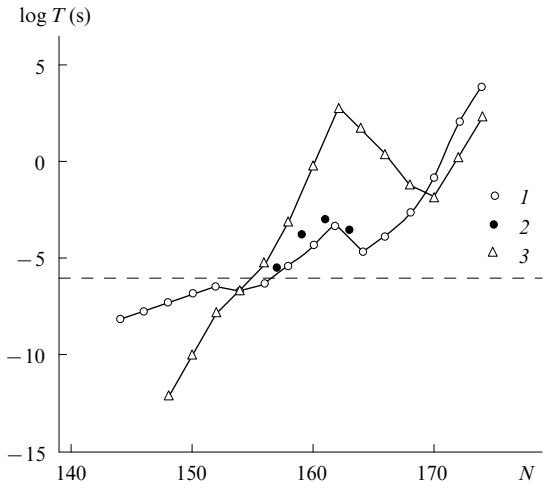


Figure 18. Comparison of the theoretically predicted (*1*) and measured (*2*) α-decay half-lives and calculated values of the spontaneous-fission half-lives (*3*) for isotopes of darmstadtium ($Z = 110$).[104]

VII. Conclusion

In a conclusion one can say that the studies of superheavy nuclei carried out for 43 years provided a lot of knowledge about them. More than 80 nuclides have been synthesized, in spite of the extremely small cross section for this process. Such properties as the decay mode, decay energy, half-life, cross section for the synthesis, have been learned. A number of these properties have been properly described and predicted by the theory before measuring them, indicating that we understand, to a large extent, the structure of these extreme nuclei, especially their shell structure.

Due to a big progress in the effectiveness of the experimental setups used in these studies, more and more subtle data is reached, in particular the spectroscopic data (*e.g.*, see Refs 109–111). This data is of a special value for theoreticians as it supplies them with subtle tests for theoretical models used in the description of superheavy nuclei.

The author would like to thank N V Antonenko, S N Dmitriev, S Hofmann, M G Itkis, Yu Ts Oganessian, K Siwek-Wilczyńska, W J Świątecki, J Wilczyński, A V Yeremin and V I Zagrebaev for helpful discussions. Support by the Polish Ministry of Science and Higher Education, Grant No. 1 P03B 042 30, and the Polish–JINR (Dubna) Cooperation Programme is gratefully acknowledged.

References

1. Yu Ts Oganessian, Yu A Lazarev, in *Treatise on Heavy-Ion Science* Vol. 4 (Ed. D A Bromley) (New York: Plenum, 1985) p. 3
2. D C Hoffman, L P Somerville, in *Particle Emission from Nuclei* (Eds D N Poenaru, M S Ivascu) (Boca Raton, FL: CRC Press, 1989) p. 1
3. E K Hulet, J F Wild, R J Dougan, L W Lougheed, J H Landrum, A D Dougan, P A Baisden, C M Henderson, R J Dupzyk, J Hahn, M Schädel, K Sümmerer, G R Bethune *Phys. Rev. C* **40** 770 (1989)
4. G T Seaborg, W D Loveland *The Elements beyond Uranium* (New York: Wiley, 1990)
5. A Ghiorso, G T Seaborg *Prog. Part. Nucl. Phys.* **31** 233 (1993)
6. S Hofmann *Rep. Prog. Phys.* **61** 639 (1998)
7. S Hofmann, G Münzenberg *Rev. Mod. Phys.* **72** 733 (2000)
8. Yu Ts Oganessian *Nucl. Phys. A* **685** 17 (2001)
9. P Armbruster *Acta Phys. Pol. B* **34** 1825 (2003)
10. G Münzenberg *Acta Phys. Pol. B* **34** 1947 (2003)
11. Yu Ts Oganessian, V K Utyonkov, Yu V Lobanov, F Sh Abdullin, A N Polyakov, I V Shirokovsky, Yu S Tsyganov, G G Gulbekian, S L Bogomolov, A N Mezentsev, S Iliev, V G Subbotin, A M Sukhov, A A Voinov, G V Buklanov, K Subotic, V I Zagrebaev, M G Itkis, J B Patin, K J Moody, J F Wild, M A Stoyer, D A Shaughnessy, J M Kenneally, R W Logheed *Phys. Rev. C* **69** 021601 (2004)
12. Yu Ts Oganessian, V K Utyonkov, Yu V Lobanov, F Sh Abdullin, A N Polyakov, I V Shirokovsky, Yu S Tsyganov, G G Gulbekian, S L Bogomolov, B N Gikal, A N Mezentsev, S Iliev, V G Subbotin, A M Sukhov, A A Voinov, G V Buklanov, K Subotic, V I Zagrebaev, M G Itkis, J B Patin, K J Moody, J F Wild, M A Stoyer, N J Stoyer, D A Shaughnessy, J M Kenneally, P A Wilk, R W Logheed, R I Il kaev, S P Vesnovsky *Phys. Rev. C* **70** 064609 (2004)
13. K Morita, K Morimoto, D Kaji, H Haba, E Ideguchi, R Kanungo, K Katori, H Koura, H Kudo, T Ohnishi, A Ozawa, T Suda, K Sueki, I Tanihata, H Xu, A V Yeremin, A Yoneda, A Yoshida, Y-L Zhao, T Zheng *Eur. Phys. J., A* **21** 257 (2004)
14. K E Gregorich, W Loveland, D Peterson, P M Zielinski, S L Nelson, Y H Chung, Ch E Düllman, C M Folden III, K Aleklett, R Eichler, D C Hoffman, J P Omtvedt, G K Pang, J M Schwantes, S Soverna, P Sprunger, R Sudowe, R E Wilson, H Nitsche *Phys. Rev. C* **72** 014605 (2005)
15. K Morita, K Morimoto, D Kaji, T Akiyama, S-i Goto, H Haba, E Ideguchi, K Katori, H Koura, H Kudo, T Ohnishi, A Ozawa, T Suda, K Sueki, F Tokanai, T Yamaguchi, A Yoneda, A Yoshidaet *J. Phys. Soc. Jpn.* **76** 043201 (2007)
16. Yu Ts Oganassian *J. Phys. G* **34** R165 (2007)
17. S G Nilsson, C F Tsang, A Sobiczewski, Z Szymanski, S Wycech, C Gustafson, I L Lamm, B Nilsson *Nucl. Phys. A* **131** 1 (1969)
18. M Brack, J Damgaard, A S Jensen, H C Pauli, V M Strutinsky, C Y Wong *Rev. Mod. Phys.* **44** 320 (1972)
19. M Bolsterli, E O Fiset, J R Nix, J L Norton *Phys. Rev. C* **5** 1050 (1972)
20. A Sobiczewski, A Gyurkovich, M Brack *Nucl. Phys. A* **289** 346 (1977)

21. P Möller, J R Nix *Nucl. Phys. A* **361** 117 (1981)
22. W D Myers, W J Swiatecki *Ark. Fys.* **36** 343 (1967)
23. K Pomorski, J Dudek *Phys. Rev. C* **67** 044316 (2003)
24. H J Krappe, J R Nix, A J Sierk *Phys. Rev. C* **20** 992 (1979)
25. S Ćwiok, J Dudek, W Nazarewicz, J Skalski, T Werner *Comput. Phys. Commun.* **46** 379 (1987)
26. V M Strutinski *Nucl. Phys. A* **95** 420 (1967)
27. V M Strutinski *Nucl. Phys. A* **122** 1 (1968)
28. D Vautherin, D M Brink *Phys. Rev. C* **5** 626 (1972)
29. J Dobaczewski, H Flocard, J Treiner *Nucl. Phys. A* **422** 103 (1983)
30. J F Berger, M Girod, D Gogny *Nucl. Phys. A* **428** 23 (1984)
31. J P Delaroche M Girod, H Goutte, J Libert *Nucl. Phys. A* **771** 103 (2006)
32. P-G Reinhard, M Rufa, J Maruhn, W Greiner, J Friedrich *Z. Phys. A* **323** 13 (1986)
33. P Ring *Prog. Part. Nucl. Phys.* **37** 193 (1996)
34. M Bender, P-H Heenen, P-G Reihard *Rev. Mod. Phys.* **75** 121 (2003)
35. Z Patyk, A Baran, J F Berger, J Dechargé, J Dobaczewski, P Ring, A Sobiczewski *Phys. Rev. C* **59** 704 (1999)
36. A Sobiczewski, K Pomorski *Prog. Part. Nucl. Phys.* **58** 292 (2007)
37. Z Patyk, A Sobiczewski, P Armbruster, K-H Schmidt *Nucl. Phys. A* **491** 267 (1989)
38. R Smolańczuk, A Sobiczewski, in *Low Energy Nuclear Dynamics (Proceedings of the XVth EPS Conference on Nuclear Physics, St Petersburg, 1995)* (Eds Yu Ts Oganessian, W von Oertzen, R Kalpakchieva) (Singapore: World Scientific, 1995) p. 313
39. Z Patyk, A Sobiczewski *Nucl. Phys. A* **533** 132 (1991)
40. Z Patyk, A Sobiczewski *Phys. Lett. B* **256** 307 (1991)
41. A Sobiczewski, F A Gareev, B N Kalinkin *Phys. Lett.* **22** 500 (1966)
42. H Meldner *Ark. Fys.* **36** 593 (1967)
43. U Mosel, W Greiner *Z. Phys.* **222** 261 (1969)
44. Z Patyk, J Skalski, A Sobiczewski, S Ćwiok *Nucl. Phys. A* **502** 591 (1989)
45. M Kowal, L Shvedov, A Sobiczewski *Int. J. Mod. Phys. E* **17** 259 (2008)
46. A Sobiczewski, I Muntian, Z Patyk *Acta Phys. Slovaca* **49** 83 (1999)
47. S Ćwiok, A Sobiczewski *Z. Phys. A* **342** 203 (1992)
48. A Sobiczewski, Z Patyk, S Ćwiok, P Rozmej *Nucl. Phys. A* **485** 16 (1988)
49. I Muntian, A Sobiczewski *Acta Phys. Pol. B* **32** 629 (2001)
50. I Muntian, Z Patyk, A Sobiczewski *Phys. At. Nucl.* **66** 1015 (2003)
51. I Muntian, S Hofmann, Z Patyk, A Sobiczewski *Acta Phys. Pol. B* **34** 2073 (2003)
52. I Muntian, Z Patyk, A Sobiczewski *Acta Phys. Hung. New Ser. — Heavy Ion Phys., 19, 139 (2004)*
53. S Liran, A Marinov, N Zeldes *Phys. Rev. C* **62** 047301 (2000)
54. I Muntian, Z Patyk, A Sobiczewski *Acta Phys. Pol. B* **32** 691 (2001)
55. W D Myers, W J Światecki *Nucl. Phys. A* **601** 141 (1996)
56. F Tondeur, S Goriely, J M Pearson, M Onsi *Phys. Rev. C* **62** 024308 (2000)
57. G Audi, O Bersillon, J Blachot, A H Wapstra *Nucl. Phys. A* **624** 1 (1997)
58. P Möller, J R Nix, W D Myers, W J Światecki *At. Data Nucl. Data Tables* **59** 185 (1995)
59. A Sobiczewski, I Muntian, O Parkhomenko, in *Structure and Dynamics of Elementary Matter (Proceedings of NATO Advanced Study Institute, Kemer, Turkey, 2003)* (Eds W Greiner, M G Itkis, J Reinhardt, M C Guclu) (Dordrecht: Kluwer Academic, 2004) p. 377
60. K H Schmidt, W Morawek *Rep. Prog. Phys.* **54** 949 (1991)
61. W Reisdorf *J. Phys. G* **20** 1297 (1994)
62. G Giardina, S Hofmann, A I Muminov, A K Nasirov *Eur. Phys. J., A* **8** 205 (2000)
63. V I Zagrebaev, Y Aritomo, M G Itkis, Yu Ts Oganessian, M Ohta *Phys. Rev. C* **65** 014607 (2001)
64. M G Itkis, Yu Ts Oganessian, V I Zagrebaev *Phys. Rev. C* **65** 044602 (2002)
65. V V Volkov *Acta Phys. Pol. B* **34** 1881 (2003)
66. A S Zubov, G G Adamian, N V Antonenko, S P Ivanova, W Scheid *Acta Phys. Pol. B* **34** 2083 (2003)
67. Y Abe, D Bouriquet *Acta Phys. Pol. B* **34** 1927 (2003)
68. W J Światecki, K Siwek-Wilczyńska, J Wilczyński *Acta Phys. Pol. B* **34** 2049 (2003)
69. V V Volkov *Phys. Part. Nucl.* **35** 797 (2004)
70. G G Adamian, N V Antonenko, W Scheid *Phys. Rev. C* **69** 044601 (2004)
71. W Loveland *Phys. Rev. C* **76** 014612 (2007)
72. K Siwek-Wilczyńska, A Borowiec, I Skwira-Chalot, J Wilczyński *Int. J. Mod. Phys. E* **17** 12 (2008)
73. A Mamdouh, J M Pearson, M Rayet, F Tondeur *Nucl. Phys. A* **644** 389 (1998) †
74. A Mamdouh, J M Pearson, M Rayet, F Tondeur *Nucl. Phys. A* **679** 337 (2001)
75. I Muntian, Z Patyk, A Sobiczewski *Acta Phys. Pol. B* **34** 2141 (2003)
76. P Möller, A J Sierk, A Iwamoto *Phys. Rev. Lett.* **92** 072501 (2004)
77. T Bürvenich, M Bender, J A Maruhn, P-G Reinhard *Phys. Rev. C* **69** 014307 (2004)
78. K Pomorski, J Dudek *Int. J. Mod. Phys. E* **13** 107 (2004)
79. R Smolańczuk, H V Klapdor-Kleingrothaus, A Sobiczewski *Acta Phys. Pol. B* **24** 685 (1993)
80. R A Gherghescu, J Skalski, Z Patyk, A Sobiczewski *Nucl. Phys. A* **651** 237 (1999)
81. A Sobiczewski, I Muntian *Nucl. Phys. A* **734** 176 (2004)
82. M Kowal, A Sobiczewski *Int. J. Mod. Phys. E* **18** 914 (2009)
83. A Sobiczewski, I Muntian *Int. J. Mod. Phys. E* **14** 409 (2005)
84. I Muntian, A Sobiczewski *Int. J. Mod. Phys. E* **14** 417 (2005)
85. A Sobiczewski, M Kowal *Phys. Scr.* **T125** 68 (2006)
86. A Dobrowolski, K Pomorski, J Bartel *Phys. Rev. C* **75** 024613 (2007)
87. P Möller, A J Sierk, T Ichikawa, A Iwamoto, R Bengtsson, H Uhrenholt, S Åberg *Phys. Rev. C* **79** 064304 (2009)
88. S Bjornholm, J E Lynn *Rev. Mod. Phys.,* **52** 725 (1980)
89. I Muntian, A Sobiczewski *Acta Phys. Pol. B* **36** 1359 (2005)
90. V E Viola Jr, G T Seaborg *J. Inorg. Nucl. Chem.* **28** 741 (1966)
91. D N Poenaru, M Ivascu *J. Phys.* **44** 791 (1983)
92. Y Hatsukawa, H Nakahara, D C Hoffman *Phys. Rev. C* **42** 674 (1990)
93. G Royer *J. Phys. G* **26** 1149 (2000)
94. K Böning, Z Patyk, A Sobiczewski, S Ćwiok *Z. Phys. A* **325** 479 (1986)
95. G A Lalazissis, M M Sharma, P Ring, Y K Gambhir *Nucl. Phys. A* **608** 202 (1996)
96. Z Lojcwski, A Baran *Z. Phys. A* **329** 161 (1988)
97. R Smolańczuk *Phys. Rev. C* **56** 812 (1997)
98. Y K Gambhir, A Bhagwat, M Gupta, A K Jain *Phys. Rev. C* **68** 044316 (2003)
99. W Zhang, J Meng, S Q Zhang, L S Geng, H Toki *Nucl. Phys. A* **753** 106 (2005)
100. A Parkhomenko, A Sobiczewski *Acta Phys. Pol. B* **36** 3095 (2005)
101. G Audi, O Bersillon, J Blachot, A H Wapstra *Nucl. Phys. A* **729** 3 (2003)
102. A H Wapstra, G Audi, C Thibault *Nucl. Phys. A* **729** 129 (2003)
103. R Smolańczuk, J Skalski, A Sobiczewski *Phys. Rev. C* **52** 1871 (1995)
104. A Sobiczewski *Acta Phys. Pol. B* **29** 2191 (1998)
105. A Ghiorso, D Lee, L P Sommerville, W Loveland, J M Nitschke, W Ghiorso, G T Seaborg, P Wilmarth, R Leres, A Wydler, M Nurmia, K Gregorich, K Czerwinski, R Gaylord, T Hamilton, N J Hannink, D C Hoffman, C Jarzynski, C Kacher, B Kadkhodayan, S Kreek, M Lane, A Lyon, M A McMahan, M Neu, T Sikkeland, W J Swiatecki, A Türler, J T Walton, S Yashita *Phys. Rev. C* **51** R2293 (1995)

† See *erratum* A Mamdouh, J M Pearson, M Rayet, F Tondeur *Nucl. Phys. A* **648** 282 (1999)

106. S Hofmann, V Ninov, F P Heßberger, P Armbruster, H Folger, G Münzenberg, H J Schött, A G Popeko, A V Yeremin, A N Andreyev, S Saro, R Janik, M Leino *Z. Phys. A* **350** 277 (1995)
107. S Hofmann, V Ninov, F P Heyberger, P Armbruster, H Folger, G Münzenberg, H J Schött, A G Popeko, A V Yeremin, A N Andreyev, S Saro, R Janik, M Leino *Z. Phys. A* **350** 281 (1995)
108. Yu A Lazarev, Yu V Lobanov, Yu Ts Oganessian, V K Utyonkov, F Sh Abdullin, A N Polyakov, J Rigol, I V Shirokovsky, Yu S Tsyganov, S Iliev, V G Subbotin, A M Sukhov, G V Buklanov, B N Gikal, V B Kutner, A N Mezentsev, K Subotic, J F Wild, R W Lougheed, K J Moody *Phys. Rev. C* **54** 620 (1996).
109. R-D Herzberg *J. Phys. G* **30** R123 (2004)
110. F P Heßberger, S Hofmann, D Ackermann, S Antalic, B Kindler, I Kojouharov, P Kuusiniemi, M Leino, B Lommel, R Mann, K Nishio, A G Popeko, B Sulignano, S Saro, B Streicher, M Venhart, A V Yeremin *Eur. Phys. J., A* **29** 165 (2006)
111. A Lopez-Martens, K Hauschild, A V Yeremin, A V Belozerov, Ch Briançon, M L Chelnokov, V I Chepigin, D Curien, O Dorvaux, B Gall, V A Gorshkov, M Guttormsen, F Hanappe, A P Kabachenko, F Khalfallah, A Korichi, A C Larsen, O N Malyshev, A Minkova, Yu Ts Oganessian, A G Popeko, M Rousseau, N Rowley, R N Sagaidak, S Sharo, A V Shutov, S Siem, A I Svirkhin, N U H Syed, Ch Theisen *Phys. Rev. C* **74** 044303 (2006)